Article

PhzA/B Catalyzes the Formation of the Tricycle in Phenazine Biosynthesis

Ekta G. Ahuja, Petra Janning, Matthias Mentel, Almut Graebsch, Rolf Breinbauer, Wolf Hiller, Burkhard Costisella, Linda S. Thomashow, Dmitri V. Mavrodi, and Wulf Blankenfeldt

J. Am. Chem. Soc., **2008**, 130 (50), 17053-17061 • DOI: 10.1021/ja806325k • Publication Date (Web): 17 November 2008

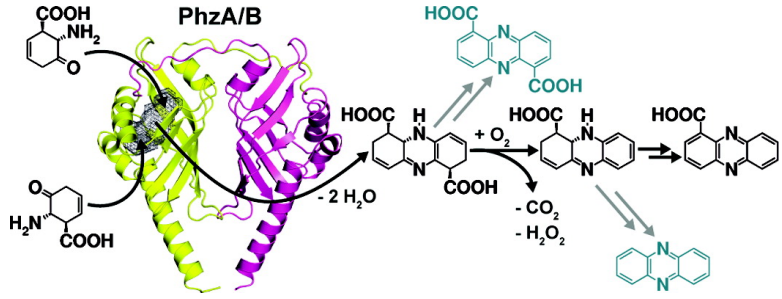

More About This Article

Additional resources and features associated with this article are available within the HTML version:

- Supporting Information
- Access to high resolution figures
- Links to articles and content related to this article
- Copyright permission to reproduce figures and/or text from this article

View the Full Text HTML

J|A|C|S
ARTICLES

Published on Web 11/17/2008

PhzA/B Catalyzes the Formation of the Tricycle in Phenazine Biosynthesis

Ekta G. Ahuja,[†] Petra Janning,[†] Matthias Mentel,[‡,§] Almut Graebsch,[‡] Rolf Breinbauer,[†,‡,§,||] Wolf Hiller,[‡] Burkhard Costisella,[‡] Linda S. Thomashow,[⊥,#] Dmitri V. Mavrodi,[⊥] and Wulf Blankenfeldt*[,†]

Max-Planck-Institute of Molecular Physiology, Otto-Hahn-Strasse 11, 44227 Dortmund, Germany, Technical University of Dortmund, Faculty of Chemistry, Otto-Hahn-Strasse 6, 44221 Dortmund, Germany, University of Leipzig, Institute of Organic Chemistry, Johannisallee 29, 04103 Leipzig, Germany, Graz University of Technology, Institute of Organic Chemistry, Stremayrgasse 16, 8010 Graz, Austria, Washington State University, Pullman, Washington 99164-6430, and USDA, Agricultural Research Service, Root Disease and Biological Control Research Unit, Pullman, Washington 99164-6430

Received August 10, 2008; E-mail: wulf.blankenfeldt@mpi-dortmund.mpg.de

Abstract: Phenazines are redox-active bacterial secondary metabolites that participate in important biological processes such as the generation of toxic reactive oxygen species and the reduction of environmental iron. Their biosynthesis from chorismic acid depends on enzymes encoded by the *phz* operon, but many details of the pathway remain unclear. It previously was shown that phenazine biosynthesis involves the symmetrical head-to-tail double condensation of two identical amino-cyclohexenone molecules to a tricyclic phenazine precursor. While this key step can proceed spontaneously *in vitro*, we show here that it is catalyzed by PhzA/B, a small dimeric protein of the Δ^5-3-ketosteroid isomerase/nuclear transport factor 2 family, and we reason that this catalysis is required *in vivo*. Crystal structures in complex with analogues of the substrate and product suggest that PhzA/B accelerates double imine formation by orienting two substrate molecules and by neutralizing the negative charge of tetrahedral intermediates through protonation. HPLC-coupled NMR reveals that the condensation product rearranges further, which is probably important to prevent back-hydrolysis, and may also be catalyzed within the active site of PhzA/B. The rearranged tricyclic product subsequently undergoes oxidative decarboxylation in a metal-independent reaction involving molecular oxygen. This conversion does not seem to require enzymatic catalysis, explaining why phenazine-1-carboxylic acid is a major product even in strains that use phenazine-1,6-dicarboxylic acid as a precursor of strain-specific phenazine derivatives.

1. Introduction

The production of phenazine pigments is among the most readily observable phenomena in bacteria, due to their intense color. This pigmentation triggered the early discovery of the blue phenazine derivative pyocyanin (1-hydroxy-5*N*-methylphenazinium betaine), which was isolated in the 1850s from wound dressings of soldiers infected with *Pseudomonas aeruginosa*.[1] Phenazines are redox-active and can reduce molecular oxygen, leading to the generation of toxic reactive oxygen species and explaining their broad-spectrum antibiotic activity. They also act as virulence factors in human infectious disease. For example, pyocyanin induces apoptosis in neutrophils, and strains of *Pseudomonas aeruginosa* defective in pyocyanin synthesis are more susceptible to immune responses in a mouse model of lung infections.[2,3] Since the lungs of nearly all victims of cystic fibrosis are chronically colonized by *P. aeruginosa* and this infection contributes significantly to the low life expectancy of these patients,[4] phenazine production may present an attractive target for pharmaceutical intervention.

Phenazines play multiple roles in the bacteria that generate them, and only recently has an understanding of these roles begun to emerge.[5] Phenazine-producing strains residing on roots can protect cultivated plants against susceptible bacterial and fungal pathogens.[6,7] In soil, phenazines can participate in iron acquisition by reducing environmental Fe^{3+} to the more soluble Fe^{2+}, and they also function in primary energy metabolism by

[†] Max-Planck-Institute of Molecular Physiology.
[‡] Technical University of Dortmund.
[§] University of Leipzig.
[||] Graz University of Technology.
[⊥] Washington State University.
[#] USDA.

(1) Fordos, J. *Recl. Trav. Soc. d'Emulation Sci. Pharm.* **1859**, *3*, 30.
(2) Allen, L.; Dockrell, D. H.; Pattery, T.; Lee, D. G.; Cornelis, P.; Hellewell, P. G.; Whyte, M. K. *J. Immunol.* **2005**, *174*, 3643–3649.
(3) Lau, G. W.; Hassett, D. J.; Ran, H.; Kong, F. *Trends Mol. Med.* **2004**, *10*, 599–606.
(4) Heijerman, H. *J. Cyst. Fibros.* **2005**, *4 Suppl 2*, 3–5.
(5) Price-Whelan, A.; Dietrich, L. E.; Newman, D. K. *Nat. Chem. Biol.* **2006**, *2*, 71–78.
(6) Giddens, S. R.; Feng, Y.; Mahanty, H. K. *Mol. Microbiol.* **2002**, *45*, 769–783.
(7) Cook, R. J.; Thomashow, L. S.; Weller, D. M.; Fujimoto, D.; Mazzola, M.; Bangera, G.; Kim, D. S. *Proc. Natl. Acad. Sci. U.S.A.* **1995**, *92*, 4197–4201.

Scheme 1. Biosynthesis of Phenazine-1-carboxylic acid (**7**)[a]

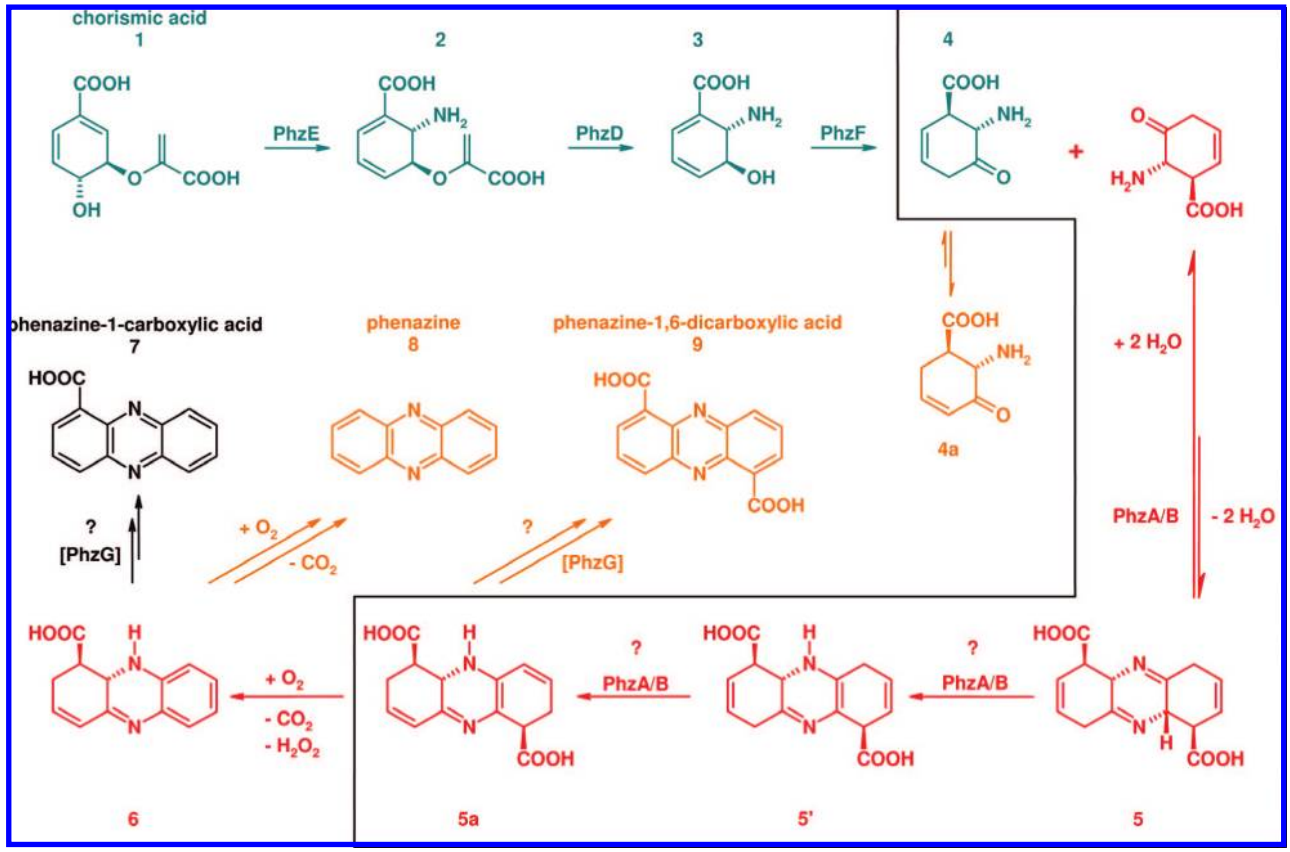

[a] Steps upstream of PhzA/B catalysis are shown in green, and intermediates discussed here are shown in red. Orange indicates byproducts. Reactions that lead to the formation of PhzA/B's product are boxed.

mediating the reoxidation of NADH and utilization of pyruvate under oxygen-limiting conditions.[8,9] In *P. aeruginosa*, pyocyanin is a signaling molecule that controls gene expression by directly activating the iron-containing transcription factor SoxR.[10] Collectively, these observations reveal some of the ways in which phenazines are exploited by their producers to interact with the environment, showing that they are more than simple secondary metabolites.

Dozens of naturally occurring phenazine derivatives have been isolated, and existing knowledge indicates that all of them originate from either phenazine-1-carboxylic acid (**7**) or phenazine-1,6-dicarboxylic acid (**9**) (Scheme 1).[11−13] These "core" phenazines are synthesized from two molecules of chorismic acid (**1**) in a pathway catalyzed by enzymes encoded in the conserved "*phz* operon". A compilation of available sequence data indicates that five Phz-enzymes are indispensable for production of **7** and/or **9** (Scheme 1 and Supporting Information Figure S1). Of these, PhzE converts **1** to 2-amino-4-desoxy-isochorismate (**2**).[14] Second, isochorismatase PhzD cleaves **2** to generate *trans*-2,3-dihydro-3-hydroxyanthranilate (**3**),[15] the last intermediate that can be isolated. In the next step, PhzF isomerizes **3**[16,17] to 6-amino-5-oxocyclohex-2-ene-1-carboxylic acid (**4**) by initiating a [1,5]-prototropic shift.[16] This ketone can undergo spontaneous dimerization by symmetrical head-to-tail double condensation *in vitro*, yielding a tricyclic phenazine precursor **5/5′/5a** that must be further oxidized to arrive at the aromatic phenazine moiety. In *Pseudomonas*, the steps past ketone condensation include oxidative decarboxylation to **6**, and core phenazine biosynthesis ends at **7**, whereas other bacteria, e.g. *Pantoea agglomerans*, generate **9** as their core phenazine.[6] Intriguingly, *in vitro* studies have revealed that none of the steps following ketone formation require enzyme catalysis, and PhzF alone can trigger conversion of **3** to **7**, albeit with low yield.[16,17] This raises questions about the function of the remaining conserved enzymes PhzA/B and PhzG. While it is relatively

(8) Hernandez, M. E.; Kappler, A.; Newman, D. K. *Appl. Environ. Microbiol.* **2004**, *70*, 921–928.
(9) Price-Whelan, A.; Dietrich, L. E.; Newman, D. K. *J. Bacteriol.* **2007**, *189*, 6372–6381.
(10) Dietrich, L. E.; Price-Whelan, A.; Petersen, A.; Whiteley, M.; Newman, D. K. *Mol. Microbiol.* **2006**, *61*, 1308–1321.
(11) Turner, J. M.; Messenger, A. J. *Adv. Microb. Physiol.* **1986**, *27*, 211–275.
(12) Laursen, J. B.; Nielsen, J. *Chem. Rev.* **2004**, *104*, 1663–1686.
(13) Mavrodi, D. V.; Blankenfeldt, W.; Thomashow, L. S. *Annu. Rev. Phytopathol.* **2006**, *44*, 417–445.
(14) McDonald, M.; Mavrodi, D. V.; Thomashow, L. S.; Floss, H. G. *J. Am. Chem. Soc.* **2001**, *123*, 9459–9460.
(15) Parsons, J. F.; Calabrese, K.; Eisenstein, E.; Ladner, J. E. *Biochemistry* **2003**, *42*, 5684–5693.
(16) Blankenfeldt, W.; Kuzin, A. P.; Skarina, T.; Korniyenko, Y.; Tong, L.; Bayer, P.; Janning, P.; Thomashow, L. S.; Mavrodi, D. V. *Proc. Natl. Acad. Sci. U.S.A.* **2004**, *101*, 16431–16436.
(17) Parsons, J. F.; Song, F.; Parsons, L.; Calabrese, K.; Eisenstein, E.; Ladner, J. E. *Biochemistry* **2004**, *43*, 12427–12435.
(18) Parsons, J. F.; Calabrese, K.; Eisenstein, E.; Ladner, J. E. *Acta Crystallogr., D: Biol. Crystallogr.* **2004**, *60*, 2110–2113.
(19) Mavrodi, D. V.; Ksenzenko, V. N.; Bonsall, R. F.; Cook, R. J.; Boronin, A. M.; Thomashow, L. S. *J. Bacteriol.* **1998**, *180*, 2541–2548.
(20) Mavrodi, D. V.; Bonsall, R. F.; Delaney, S. M.; Soule, M. J.; Phillips, G.; Thomashow, L. S. *J. Bacteriol.* **2001**, *183*, 6454–6465.
(21) Haagen, Y.; Gluck, K.; Fay, K.; Kammerer, B.; Gust, B.; Heide, L. *ChemBioChem* **2006**, *7*, 2016–2027.

clear that the FMN-dependent PhzG is involved in one of the terminal oxidation reactions,[18] the function of PhzA/B is not obvious. Working with *E. coli* expressing fragments of the *phz* operon, it was shown that this enzyme, while not required for phenazine biosynthesis, increases the efficiency of the pathway severalfold.[14,19] Deletion of the gene in *P. agglomerans* led to complete abrogation of phenazine biosynthesis,[6] arguing for an absolute *in vivo* requirement, and Parsons et al. hypothesized that it may be involved in the dimerization step that generates the phenazine tricycle.[17] This could explain why phenazine production is so prominent in the pseudomonads, which, in contrast to other phenazine producing bacteria, possess two adjacent, highly homologous copies of this gene, *phzA* and *phzB* (approximately 80% amino acid identity, Figures S1 and S2).[19,20] Two copies of the gene are also found in *Streptomyces cinnamomensis*, but they are not neighbored.[21] Because of the high similarity of PhzA, PhzB, and the corresponding proteins in other strains, they are termed "PhzA/B" here when not referring to one of the two specific *Pseudomonas* genes.

Fold prediction indicated that PhzA/B belongs to the Δ^5-3-ketosteroid isomerase (KSI)/nuclear transport factor 2 (NTF2) family.[22] Because members of this family participate in a plethora of reactions, serve in nuclear transport processes, and act as assembly platforms for larger protein complexes, it is not possible to deduce the function of PhzA/B from this fold relationship alone. We have therefore developed biochemical assays and performed crystal structure analysis of PhzA/B from *Burkholderia cepacia* R18194 to learn more about the role of this protein in phenazine biosynthesis.

2. Results

2.1. PhzA/B Catalyzes the Condensation Step in Phenazine Biosynthesis. In order to identify if and which of the steps in phenazine biosynthesis PhzA/B catalyzes, we applied different ratios of PhzF and PhzA/B from *B. cepacia* to **3** and employed HPLC-coupled mass spectrometry to follow the turnover of **3**, ketone **4**, tricyclic intermediate **5/5′/5a**, the product of its oxidative decarboxylation **6**, and the end product **7** in addition to some minor species including probably the less reactive vinyl ketone **4a** and the byproducts **9** and phenazine (**8**) (Figure 1a, b, and e and Figures S3−S9). The same intermediates were also observed with Phz-enzymes from *Pseudomonas*, showing that phenazine biosynthesis follows the same pathway in both species.

Increasing concentrations of PhzA/B led to greater amounts of condensation product **5/5′/5a**, which also peaked at earlier times (Figure 1a). Simultaneously, ketone **4** and its isomer **4a** were drastically decreased (Figure 1b and Figure S5a). To determine the structure of the unstable condensation product, we conducted HPLC-coupled NMR experiments, which reveal that this product is the nonsymmetrical molecule **5a**, containing four conjugated double bonds (Figure 1c, Figures S10 and S12). This shows that condensation is accompanied by rearrangement reactions that may be required to stabilize double imine **5**, which probably is water-sensitive, against back-hydrolysis to **4**.

PhzA/B could fulfill two different roles in the reaction cascade leading from **4** to **5a**. First, PhzA/B could utilize ketone **4** as its substrate and catalyze condensation to **5**, followed by spontaneous rearrangement to **5a**. Second, if condensation already takes place in PhzF as we previously speculated,[16] PhzA/B could isomerize **5** to **5a** by acid/base catalysis. In this case, **4** would not be released from PhzF and the ketones **4** and **4a** detected by HPLC-MS would stem exclusively from back-hydrolysis of **5**. We therefore assessed the incorporation of ^{18}O into **4** and **4a** in reactions carried out in $H_2{}^{18}O$. Only minor incorporation of the label was found shortly after initiation of the reaction, when ketone concentrations are highest (Figure S6), thus demonstrating that PhzF indeed releases ketone **4** as its product. This suggests that PhzA/B catalyzes the subsequent condensation reaction, which is also supported by an experiment in which PhzA/B was added after PhzF had already fully depleted its substrate **3** and the concentration of the condensation product **5a** was again declining (Figure S7). Here, a new maximum of **5a** developed, indicating that PhzA/B utilizes free ketone **4** as its substrate. It also shows that formation of **5a** does not involve the substrate of PhzF **3** in, for example, a reaction condensing one molecule of **3** and one molecule of ketone **4**.

2.2. The Product of PhzA/B Is Oxidation Sensitive. Mass spectrometry reveals that **5a** undergoes oxidative decarboxylation to give a species that most likely is the partially aromatized intermediate **6**. To identify the electron acceptor of this and the following reactions, we monitored dissolved O_2 with a Clark electrode. This shows that oxygen is depleted once PhzF begins turnover of **3** and that O_2-depletion is accelerated with increasing concentrations of PhzA/B (Figure 1d). With a carbon dioxide selective electrode, it was also possible to confirm the release of CO_2 (Figure S13). Following the reaction by HPLC-MS shows that intermediate **6** forms earlier in the presence of PhzA/B but that its overall quantity does not change significantly (Figure 1e), which may be a consequence of limited oxygen availability in the reaction mixture. Because efficient oxygen consumption is already triggered by PhzF alone and because the higher rate of depletion likely results from PhzA/B's acceleration of the step preceding oxidative decarboxylation, we hypothesize that oxidation of **5a** to **6** proceeds without enzymatic catalysis. This would explain why **7** is found as a major byproduct even in strains that utilize **9** rather than **7** as a precursor of their strain-specific phenazines.[6]

Experiments with chelating reagents show that oxygen consumption does not depend on metal ions (Figure S14), leaving the question about oxygen activation unanswered. In reactions with low initial amounts of **3**, approximately half of the depleted oxygen was recovered by addition of catalase, demonstrating the generation of H_2O_2, which was also detectable with Amplex Red (Figure S15).

While details of the spontaneous conversion of **5a** to **6** remain elusive, it is apparently propagated by the irreversibility of decarboxylation and by the stability gained in generating the aromatic π-system of **6**. In this regard, phenazine biosynthesis is reminiscent of pathways involving oxidative cascades, in which cyclization is followed by oxidation that is often uncatalyzed and restores aromaticity on the substrate.[23] More

(22) Ahuja, E. G.; Mavrodi, D. V.; Thomashow, L. S.; Blankenfeldt, W. *Acta Crystallogr., D: Biol. Crystallogr.* **2004**, *60*, 1129–1131.
(23) Dorrestein, P.; Begley, T. P. *Bioorg. Chem.* **2005**, *33*, 136–148.
(24) Kis, K.; Kugelbrey, K.; Bacher, A. *J. Org. Chem.* **2001**, *66*, 2555–2559.
(25) Burgi, H. B.; Dunitz, J. D.; Lehn, J. M.; Wipff, G. *Tetrahedron* **1974**, *30*, 1563–1572.
(26) Kim, S. W.; Cha, S. S.; Cho, H. S.; Kim, J. S.; Ha, N. C.; Cho, M. J.; Joo, S.; Kim, K. K.; Choi, K. Y.; Oh, B. H. *Biochemistry* **1997**, *36*, 14030–14036.
(27) Doublie, S. *Methods Enzymol.* **1997**, *276*, 523–530.
(28) Wolf, C.; Liu, S. L.; Mei, X. F.; August, A. T.; Casimir, M. D. *J. Org. Chem.* **2006**, *71*, 3270–3273.
(29) Smallcombe, S. H.; Patt, S. L.; Keifer, P. A. *J. Magn. Reson. A* **1995**, *117*, 295–303.

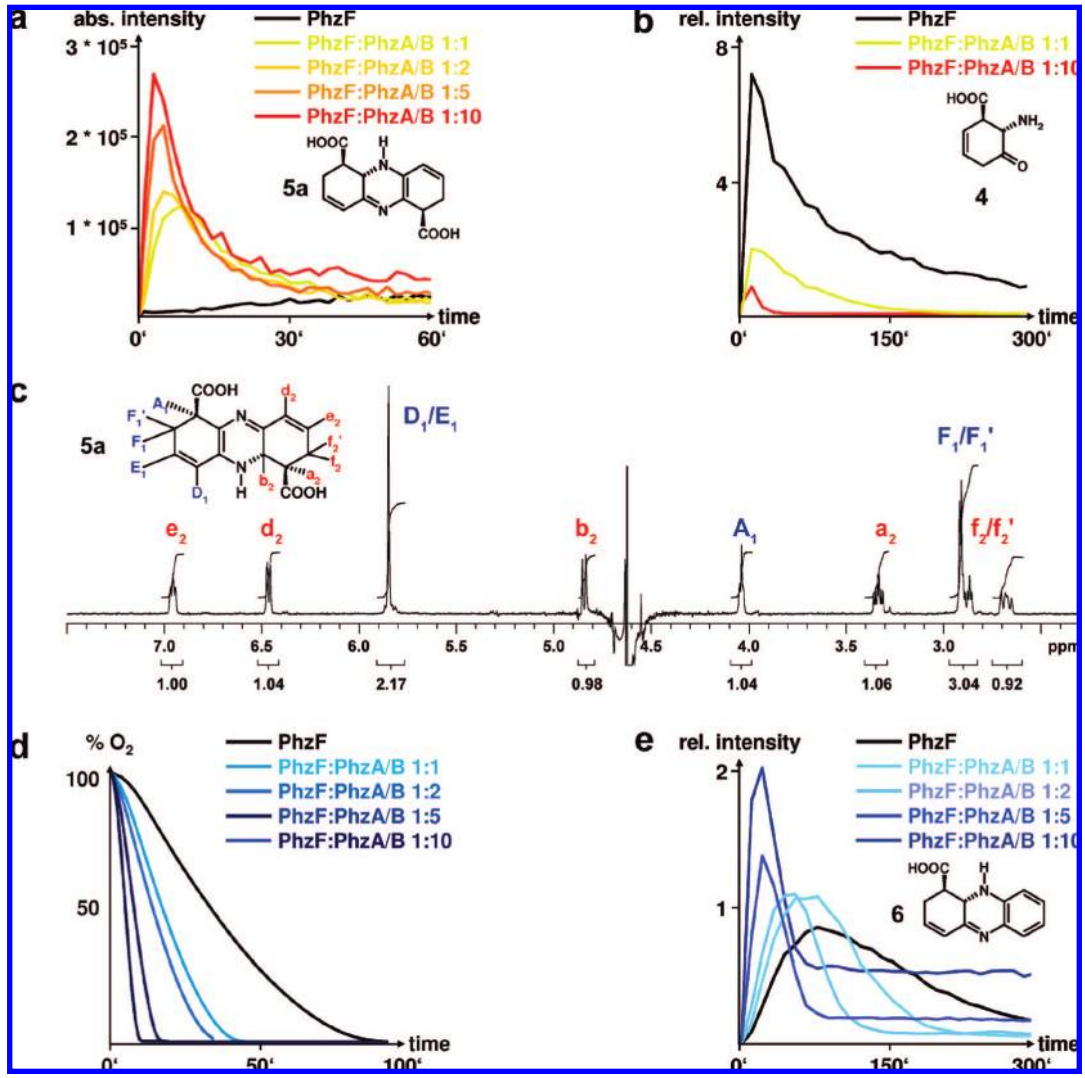

Figure 1. Functional characterization of PhzA/B. (a) Influence of increasing concentrations of PhzA/B on ketone condensation product **5a**, observed by HPLC-MS without column separation. The initial concentration of **3** was 0.1 mM, and PhzF was applied at 1 μM. (b) Depletion of ketone **4** by PhzA/B, observed by HPLC-MS with column separation. The initial concentration of **3** was 1 mM, and turnover was initiated with 1 μM PhzF. Note the different time scales of (a) and (b). (c) ^{1}H NMR and assignment of ketone condensation product **5a** recorded by HPLC-coupled NMR spectroscopy. (d) Depletion of oxygen during turnover of 1 mM **3** in the presence of increasing amounts of PhzA/B. Reactions were initiated with 1 μM PhzF. (e) Influence of PhzA/B on **6** observed by HPLC-MS with column separation.

research will be needed to understand this step in phenazine biosynthesis, but it seems that **5a** is primed to lose CO_2 due to the conjugated π-system in the β-position to the carboxylate group.

The ability to accelerate oxygen depletion was used as an activity test for assessing the effect of mutations in PhzA/B (Table S4).

2.3. PhzA/B Is a Dimeric KSI/NTF2 Protein. To gain further insight into the role of PhzA/B, we have determined the crystal structure of the *B. cepacia* enzyme in two different crystal forms with 1.65 and 2.2 Å resolution, respectively (Figure 2 and Table S2). PhzA/B indeed possesses a KSI/NTF2-fold, but the dimer features an arm-exchange not observed in related protein structures (listed in Table S3). Consequently, the C-terminus of each chain contributes to the formation of the active center of the neighboring monomer (Figure 2). Residues of the C-terminus refine to higher B-factors than the rest of the structure and could not be traced in some of the data sets collected for this study (from R160 or D161 to S165 in the higher or lower resolution crystal form, respectively; Figure S18). Since the active site is fully shielded from the solvent when all residues of the C-terminus are present, we hypothesize that the C-terminus acts as a flexible lid that controls access to the active site. It is also critical for activity and stability (Table S4): while introduction of a stop codon at position 164 yields a fully active enzyme, truncation at residue 162 impairs activity slightly and shortening the protein to 159 residues renders PhzA/B nonfunctional, which is expected, since R160 participates in ligand binding (see below). Truncation at P156 results in a protein that is no longer stable. PhzA/B also possesses flexible α-helical N-termini that point out of the fold core and are too mobile to be fully traced. Their function is not obvious.

The two active sites of the dimer reside in large cavities lined mainly by aromatic and hydrophobic residues together with several polar side chains (Figure 2b−d), whose importance is highlighted by their high degree of conservation (Figure S2). Two acetate ions from the crystallization buffer bind to R41 and R160* in the active site of the apo structure (* indicates the second monomer). Their methyl groups point in opposite parallel directions, hinting at the position and approximate

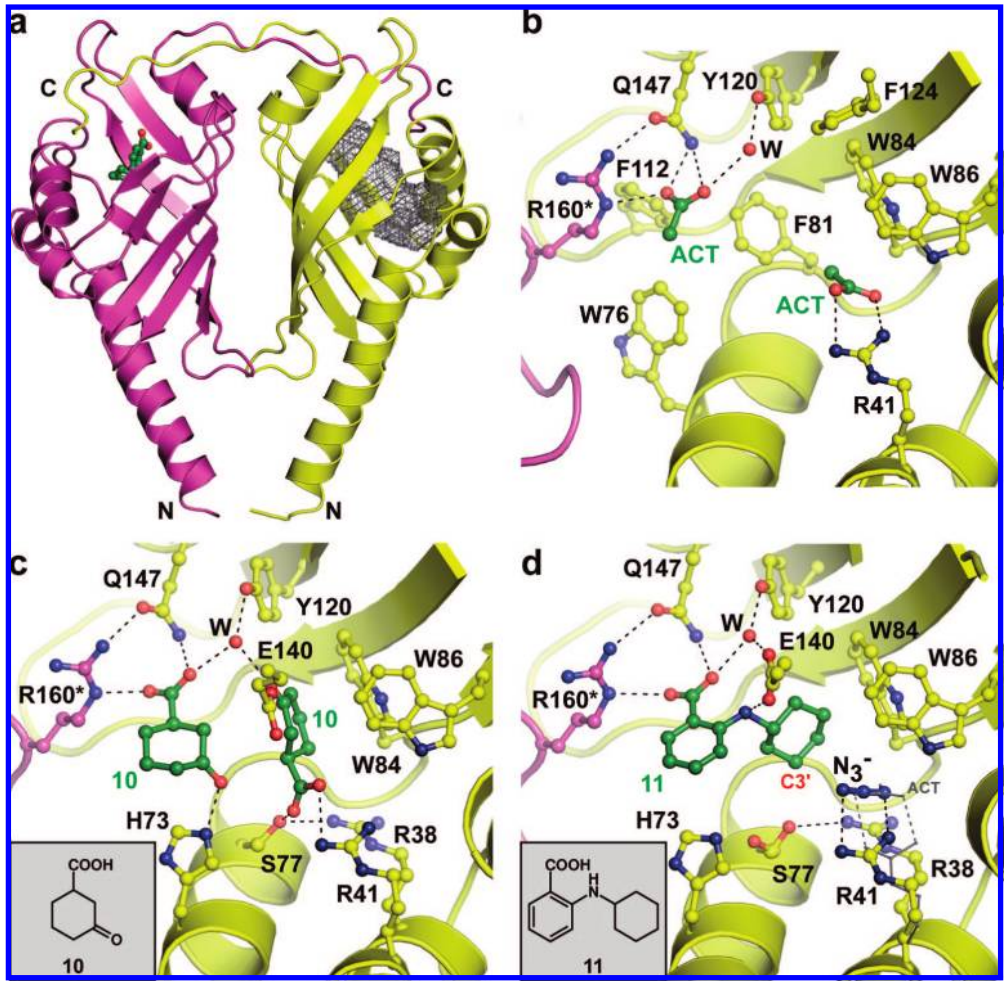

Figure 2. Crystal structure of *Burkholderia cepacia* PhzA/B. (a) Overall structure of the dimer. N- and C-termini are indicated. Compound **11** is shown in one of the active centers. The active site cavity is shown as a gray mesh in one of the monomers. (b) Binding of two acetate ions (ACT) in the apo structure with emphasis on nonpolar residues lining the active center. (c) Binding of **10** with emphasis on conserved polar residues of the active center. (d) Binding of **11** and azide. Thin gray lines indicate the shifted position of acetate and R41 in the active center of the second monomer.

orientation with which substrate molecules bind (Figure 2b). Because this information is not sufficient to derive the details of the interaction between the protein and its natural ligands and because these ligands are too unstable to be isolated for crystallographic experiments, we used isothermal titration calorimetry (ITC) to test substrate analogues and synthetic mimics of the product of PhzA/B (Figures S16, S17, S19, and Table S1). While none of the analogues of ketone **4** showed binding in ITC, it was still possible to obtain complexes with **3** and with 3-oxocyclohexanecarboxylic acid (**10**) by soaking (Figure 2c and Figure S19). The carboxylate group of these ligands interacts either only with R41 in the form of a salt bridge (complex with **3**, Figure S19a) or with R41 and S77 simultaneously (complex with **10**, Figure 2c and Figure S19b). It is possible that this ambivalence is required in the catalytic cycle of PhzA/B (Figure 3). The 2-amino and 3-oxo/hydroxy groups form hydrogen bonds to E140. E140, S77, and R41 adopt multiple conformations in the various structures presented here, and this mobility seems important for catalysis (Figure 3a, Scheme 2). The 3-oxo/hydroxy groups of **3** and **10** also bind to Y120 via a water molecule. Interestingly, even if a racemic mixture of **10** was used, only the (*R*)-form binds to the active center, and C1 of **3** is distorted toward (*R*)-configured sp^3-hybridization (Figure S19a), in both cases exhibiting the expected stereochemistry at C1 of ketone **4**. While only one molecule of **3** binds to the active center, a second, weakly bound molecule of **10**, also in the (*R*)-configuration, replaces acetate at R160*, where it also coordinates Q147 and, through the same water molecule as the first molecule of **10**, Y120. Its 3-oxo group forms a hydrogen bond to H73.

Of the product analogues, the best compounds have affinities between 2 and 25 μM (Figure S17 and Table S1). Since all of the analogues investigated by crystallography displayed a similar binding mode (Figure S20), only 2-(cyclohexylamino)benzoic acid (**11**) is discussed here (Figure 2d and Figure S19c). Like the second molecule of **10**, the carboxylate group of **11** replaces acetate at R160*, while the other acetate is pushed to the side together with R41 in one of the active centers or replaced by azide from the crystallization buffer in the other (Figures 2d and 3a). Further, the amino bridge in **11** forms a hydrogen bond to the side chain of E140, indicating how an imine intermediate could interact with PhzA/B. The planes of the two rings are tilted such that substitution with carboxylate at C3′ of the cyclohexyl moiety for interaction with R41 requires a chiral center with the same configuration as C1 in ketone **4**. This explains why none of the synthetic ligands with two carboxylate groups investigated here show binding to PhzA/B (Figure S16).

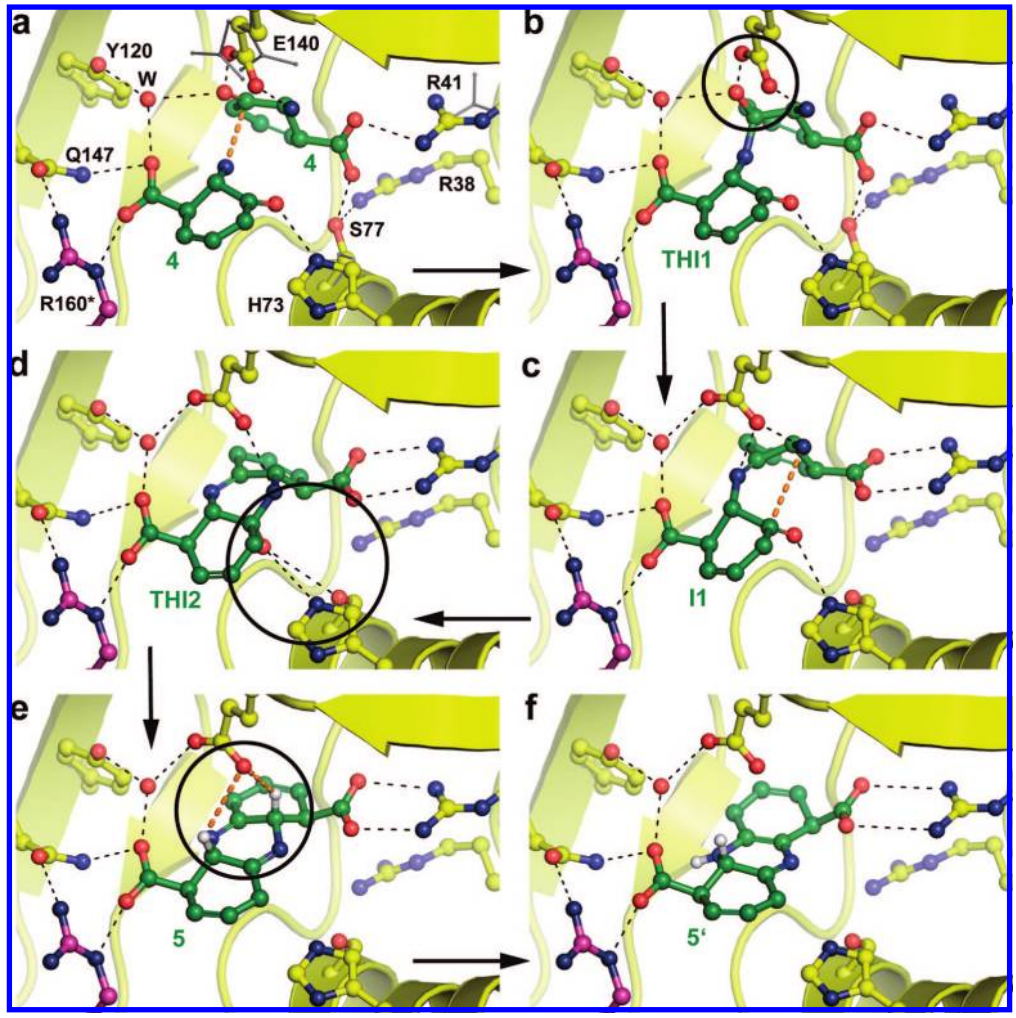

Figure 3. Catalytic proposal for PhzA/B. The initial position of the two ketone substrate molecules **4** in (a) is based on the complexes with **3** and **10**. Gray sticks show the conformation of R41, S77, and E140 found in other data sets (Table S2). Orange dashes mark nucleophilic attacks; circles indicate catalysis by proton transfer. THI1/2, first and second tetrahedral intermediate; I1, first imine.

3. Discussion

Our data show that PhzA/B catalyzes the formation of the phenazine tricycle from two identical precursors, a reaction that also proceeds without catalysis *in vitro*. Why does the *phz* operon contain the PhzA/B enzyme if it is apparently not essential for phenazine biosynthesis? The answer may be that the uncatalyzed condensation requires a bimolecular step, for which the reaction rate declines exponentially upon dilution. Accordingly, the uncatalyzed reaction is very slow at low concentrations of **3** and catalysis by PhzA/B leads to great acceleration as well as, within the time frame of the experiments summarized here, overall yield, since side reactions are prevented. On the other hand, only little acceleration results when the initial amount of substrate is higher than 1 mM, indicating that significant product forms uncatalyzed under these conditions (Figure S8). In the bacterial cell, phenazine biosynthesis is coupled to the shikimate pathway, which implies that the intracellular concentration of phenazine precursors never reaches millimolar levels. Under these circumstances, breakdown of the reactive ketone **4** by, for example, oxidation or reaction with free amino groups of proteins must be avoided, explaining why PhzA/B catalysis is required *in vivo*. This is, for example, demonstrated by the complete abrogation of phenazine production after deletion of the gene in *Pantoea agglomerans* Eh1087.[6] In this respect, the function of PhzA/B is reminiscent of the otherwise unrelated lumazine synthase in riboflavin biosynthesis, which catalyzes a similar condensation reaction that can also proceed spontaneously.[24]

The crystal structures presented here, together with mutagenesis data (Table S4), allow us to propose a catalytic mechanism in which PhzA/B accelerates multiple reactions, leading from ketone **4** to the rearranged condensation product **5a** (Scheme 2 and Figure 3). The complex with **3** shows that the catalytic cycle is initiated by binding of the first ketone molecule to R41 and possibly also to S77 by its carboxylate group. Interaction of the 2-amino and 3-oxo groups with E140 positions the ring. Next, the second substrate molecule binds to R160* and H73, as seen in the complex with **10**. This is also expected to anchor the mobile C-terminus, which would then shield the active site from the solvent. The rings of the two ketones are positioned at a nearly perpendicular angle, and the molecules approach each other such that a nucleophilic attack by the 2-amino group of the second ketone at C3 of the first can start the condensation reaction (Scheme 2a and Figure 3a). The small structural alterations required for this attack to follow a Bürgi−Dunitz trajectory[25] seem easily achievable due to the mobility of R41, S77, and E140 mentioned above. Catalysis is brought about by the indispensible E140, which protonates the negatively charged

Scheme 2. Catalytic Proposal for PhzA/B Showing the Most Important Proton Transfer Reactions[a]

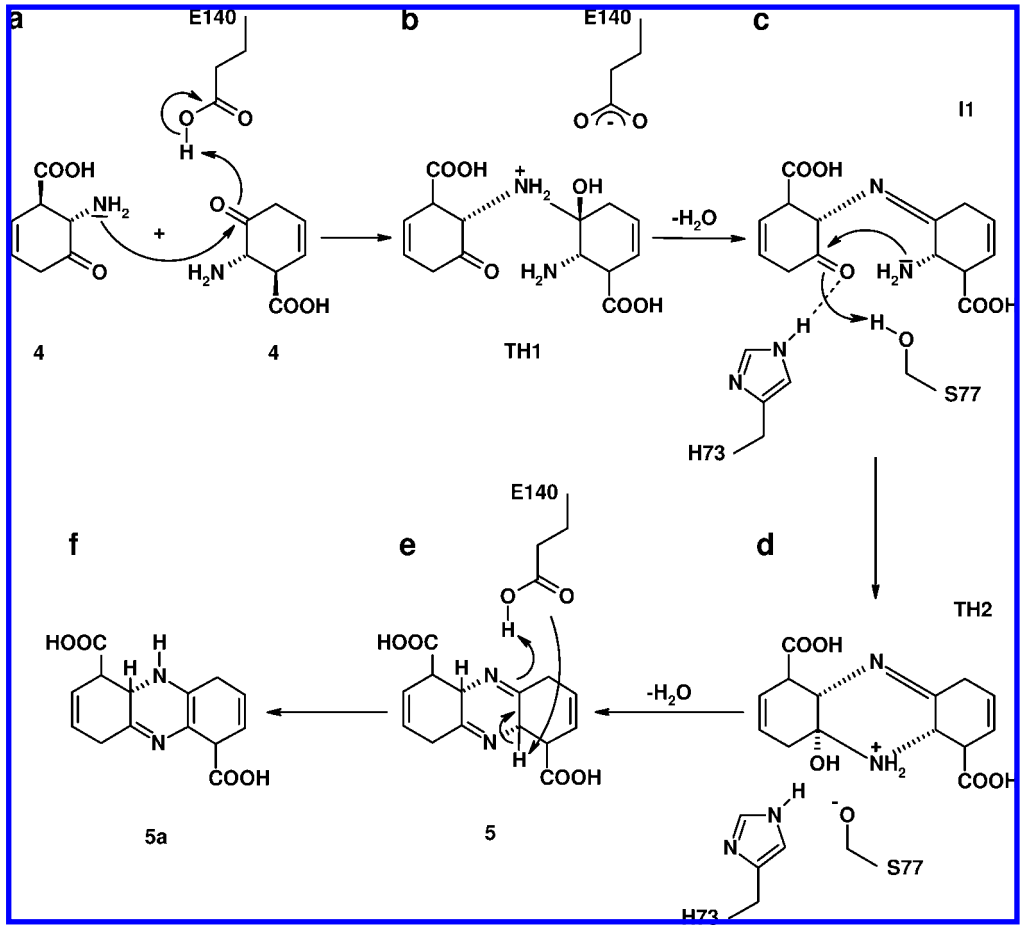

[a] THI1/2, first and second tetrahedral intermediate; I1, first imine. The stages shown here correspond to those shown in Figure 3.

oxygen atom of the resulting tetrahedral intermediate (Scheme 2b and Figure 3b). The environment of E140 is hydrophobic, which will increase its pK_a, as in other members of the KSI/NTF2 family, who often also possess a catalytically important residue at this position or in the immediate vicinity.[26] Loss of water concludes formation of the first imine bond, which is in the less favored *cis* conformation because of the relative initial orientation of the substrate molecules. As a consequence of this first condensation reaction, the 2-amino group of the first ketone comes closer to the carbonyl group of the second, triggering formation of the tricycle (Scheme 2c and Figure 3c). This second, intramolecular condensation will be strongly facilitated and may not require catalysis, but the model suggests that the negative charge of the associated tetrahedral intermediate is neutralized by H73 and S77 (Figure 3d). To participate in catalysis, S77 must adopt the second conformation observed in the complex with **11**, and the positive charges of the nearby R38 and R41 probably decrease its pK_a for this task. While mutation of H73 had only a minor impact on activity, S77 was absolutely required, but it is unclear at present whether this is due to reduced affinity for the first substrate molecule or because of an incapacity to act in catalysis. Interestingly, H73 and S77 are both substituted with leucine in the PhzA proteins of *Pseudomonas*, and PhzA was indeed found inactive in our assays (Figure S9). We hypothesize that PhzA and PhzB from *Pseudomonas*, due to their high similarity, can form heterodimers with only one catalytically competent active center. This could increase the efficiency of phenazine biosynthesis *in vivo* because of the peculiarity that the condensation step requires two identical substrate molecules. The homodimeric *B. cepacia* PhzA/B protein possesses four binding sites for ketone **4**, two of which, according to the crystal structures presented here, have high affinity but are located in the separate active centers. As a consequence, the high-affinity binding site of the second active center reduces the effective concentration of ketone at the second, lower affinity substrate binding site of the first active center, leading to a decreased condensation rate at the substrate concentrations anticipated in the cell.

While the present data do not allow us to unequivocally rule out that the two imine bonds form simultaneously, the model indicates that PhzA/B could also participate in the final "maturation" of double imine **5** by catalyzing the shift of one of the protons in the α-position to the imine bonds to give **5′** (Schemes 1 and 2e, f and Figure 3e, f). The proximity and mobility of E140 make this residue ideally suited for this function. Rearrangement within PhzA/B is advantageous, since contact with the solvent is avoided. However, an intermediate **5′** cannot be observed, probably because the final proton shifts that convert **5′** to **5a** are facile due to the stability gained by conjugating the four double bonds.

The observation that oxygen participates in the spontaneous oxidative decarboxylation of the product of PhzA/B is a new aspect of phenazine biosynthesis. It suggests that phenazine production is limited to aerobic lifestyle, which is in contradiction to a recent study demonstrating that *P. aeruginosa* still produced pyocyanin when oxygen was depleted.[9] However, the

nonenzymatic nature of the oxidative decarboxylation makes it possible that other chemical oxidants participate in this process.

The detection of phenazine-1,6-dicarboxylic acid (**9**) and unsubstituted phenazine (**8**) as byproducts demonstrates that **5a** can follow several routes to gain aromaticity. These involve either spontaneous oxidative decarboxylation, leading to **8** when occurring twice, or oxidation without loss of CO_2, leading to **9**. The later implies participation of a cofactor-dependent oxidase, probably the FMN-containing PhzG of the *phz* operon, and we suggest that bacteria that utilize **9** for the production of strain-specific phenazine derivatives show different relative activities of the enzymes PhzA/B and PhzG.

Because of the requirement of PhzA/B *in vivo*, the synthetic probes used for functional analysis in this study could act as lead compounds against phenazine biosynthesis in infectious disease. Using the complex with **11** as a guide, we are currently synthesizing improved inhibitors of PhzA/B.

4. Conclusion

The formation of the tricycle in phenazine biosynthesis involves the condensation of two identical amino-cyclohexenone precursors **4** to a double imine **5**. While this bimolecular reaction does not require catalysis *in vitro*, it is catalyzed by the small dimeric KSI/NTF-2 protein PhzA/B *in vivo*, which acts as an acid/base catalyst and significantly increases the reaction rate at the low substrate concentration expected to exist in the bacterial cell. Condensation is accompanied by rearrangement reactions to yield an asymmetric molecule with four conjugated double bonds **5a**, thereby preventing back-hydrolysis to **4**. The rearranged condensation product is oxidation-sensitive and undergoes oxidative decarboxylation in a nonenzymatic reaction involving dissolved oxygen, explaining why phenazine-1-carboxylic acid (**7**) and not phenazine-1,6-dicarboxylic acid (**9**) is the major product of phenazine biosynthesis. However, the detection of unsubstituted phenazine (**8**) and of phenazine-1,6-dicarboxylic acid (**9**) in our *in vitro* experiments indicates that condensation product **5a** can follow different oxidative pathways to gain aromaticity, making phenazine biosynthesis promiscuous to a certain extent.

5. Materials and Methods

For full experimental details, refer to the online Supporting Information.

5.1. Cloning, Protein Expression and Purification, and Mutagenesis. Proteins were expressed from pET15b in *E. coli* Rosetta2 pLysS (Merck Biosciences). Seleno-methionine labeling was achieved by suppression of methionine biosynthesis in M9 media.[27] Mutations were introduced with the QuikChange II XL system (Stratagene). Purification was achieved by Ni^{2+}-affinity chromatography followed by a size-exclusion step.

5.2. Synthesis of 2-(Cyclohexylamino)benzoic acid (11). Compound **11** was synthesized by copper-catalyzed amination of 2-bromobenzoic acid with cyclohexylamine following a published protocol[28] and purified by flash chromatography.

5.3. Isothermal Titration Calorimetry. Calorimetric experiments were carried out with a VP-ITC system (MicroCal LLC) by titrating 1 mM ligand in 20 mM Tris-HCl pH 8, 150 mM NaCl to 0.1 mM PhzA/B in the same buffer at 25 °C. Data were analyzed with Origin (OriginLab Corporation).

5.4. Crystallization, Data Collection, Structure Solution, and Refinement. Initial crystallization conditions were sought at 20 °C with screens "The Classics" and "The PEG Suite" (Qiagen), using a protein concentration of 15 mg/mL. The optimized setup consisted of a 1 μL + 1 μL hanging drop at 12 °C equilibrated against a 500 μL reservoir of 16−20% (w/v) PEG 3350, 0.2 M NH_4-acetate, and 0.1 M Bis-Tris pH 6.1−6.7. Cryoprotection was achieved by briefly washing in mother liquor with PEG 3350 increased to 25% (w/v). Both crystal forms appeared under similar conditions and sometimes in the same drop, with the $C222_1$ crystals having a tendency to form at lower pH and lower precipitant concentration. Complexes were obtained by overnight soaking of the $P3_221$ crystals in mother liquor supplemented with 10 mM 2-(cyclohexylamino)benzoic acid (**11**) or 50 mM of the other ligands. *trans*-2,3-Dihydro-3-hydroxyanthranilate (**3**) was a kind gift from DSM Anti-Infectives, and racemic 3-oxocyclohexanecarboxylic acid (**10**) was from Sigma.

All data were collected on beamline X10SA of the Swiss Light Source (Villigen, Switzerland). The structure was solved from selenium-edge SAD data of a $P3_221$ crystal. The $C222_1$ structure was solved by molecular replacement. Full data collection and refinement statistics are shown in Table S2.

5.5. HPLC-Coupled Mass Spectrometry. Turnover of **3** (0.1−5 mM) in 50 mM Tris-HCl pH 7.5, supplemented with 10 μM caffeine as internal reference, was initiated with 1 μM PhzF and varying concentrations of PhzA/B at 10 °C. Reaction mixtures were analyzed by an Agilent 1100 HPLC system coupled to a diode array detector and an LTQ mass spectrometer (Thermo Electron Corporation) operated with atmospheric pressure chemical ionization in the positive mode.

1-μL samples were injected at either 11-min intervals and separated on a Waters Atlantis dC18 column (3 μm, 4.6 × 100 mm) or at 2-min intervals without column separation. The column was developed with a H_2O/acetonitrile gradient supplemented with 0.1% formic acid. 2.5 μL injections were applied in $H_2{}^{18}O$ labeling experiments. $H_2{}^{18}O$ was from Isotec.

Mass spectra were analyzed with Xcalibur (Thermo Electron Corporation) by referencing the peak area of each species to that of caffeine except in the case of experiments without column separation, where caffeine could not be quantified.

5.6. Online HPLC-Coupled ^{1}H NMR Spectroscopy. Experiments were carried out on a Varian Inova 600 MHz NMR spectrometer equipped with a pulse field gradient triple resonance LC probe head coupled to a Varian ProStar HPLC system. A ProntoSIL 120-5-C18-Aq 5 μm column (Bischoff Analysentechnik) was used to separate 100 μL of a reaction mixture (100 mM of **3**, 10 μM PhzF and 20 μM PhzA/B in 250 mM Tris-HCl pH 7.5) after 40 min of incubation. The column was developed in a gradient of degassed H_2O and acetonitrile (Riedel-deHaën Chromasolv, HPLC-NMR grade) supplemented with 0.1% TFA. On-flow and stop-flow experiments were carried out with WET suppression of the water and acetonitrile resonances.[29]

5.7. Oxygen Measurements and H_2O_2 and CO_2 Detection. Oxygen consumption was followed with a Clark electrode in a sealed chamber at 25 °C. Turnover of 1 mM of **3** in 50 mM Tris-HCl pH 7.5 was initiated with 1 μM PhzF and varying amounts of PhzA/B (1−10 μM). Mutants of PhzA/B were assessed at 10 μM. The influence of metal ions was tested with Chelex beads or EDTA. H_2O_2 production was probed with catalase or Amplex Red (Invitrogen).

The generation of CO_2 was tested with a selective electrode (Microelectrodes Inc.). One millimolar **3** was reacted with 3 μM PhzF and varying amounts of PhzA/B.

Acknowledgment. We thank Roger Goody for his generous support of this project. Petra Geue and Christiane Pfaff are acknowledged for excellent technical assistance, Georg Holtermann for reviving a homemade Clark electrode from the 1970s, Aybike Yektaoglu for synthesizing 2-(cyclohexylamino)benzoic acid, and Bernhard Griewel for measuring NMR spectra. DSM Anti-Infectives B.V. (Delft, The Netherlands) made a generous contribution of pure *trans*-2,3-dihydro-3-hydroxyanthranilate. We thank the X-ray communities of the Max-Planck-Institutes of Molecular Physiology (Dortmund, Germany) and for Medical Research (Heidelberg, Germany) for collecting diffraction data at the Swiss Light Source of the Paul Scherrer Institute (Villigen, Switzerland), which gave us generous access and support for beamline X10SA. This project was sponsored in part by grants of the Bioband of the University of Dortmund to R.B. and W.B. and of the Deutsche Forschungsgemeinschaft to W.B. (BL587).

Supporting Information Available: . Full experimental details, protein sequence data, additional HPLC-coupled mass spectrometry data, 2D-NMR spectra of ketone condensation product **5a**, CO_2-detection, oxygen depletion experiments, H_2O_2 detection, results of ITC experiments, $2F_OF_C$ electron density of the C-termini in $P3_221$ and $C222_1$ crystals, $|F_OF_C|$ electron density of ligands, additional structural presentations, crystallographic data collection and refinement statistics, list of related protein structures, and activity of mutants. This material is available free of charge via the Internet at http://pubs.acs.org.

JA806325K